PAPER

Check for updates

Contrasting thermoresponsiveness of stereoisomers of a dense 1,2,3-triazole polymer carrying amide side chains†

Koji Okuno,[a] Junji Miura,[a] Shota Yamasaki,[a] Masaki Nakahata,[a] Yuri Kamon[b] and Akihito Hashidzume [ID] *[a]

Since thermoresponsive polymers are an important class of smart polymer materials, it is an important subject of investigation to develop thermoresponsive polymers with a new polymer backbone for expanding their potential. Recently, we synthesized poly(*N*-ethyl-*N*-methyl-4-azido-5-hexynamide) (poly(**ME**)) by copper(I)-catalyzed azide–alkyne cycloaddition (CuAAC) polymerization as a new lower-critical-solution-temperature (LCST) type thermoresponsive polymer. In this study, we synthesized two types of stereoregular poly(**ME**) (*i.e.*, isotactic and syndiotactic) by CuAAC polymerization of **ME** dimers of the *R*- and *R*-isomers, and the *R*- and *S*-isomers, respectively, and investigated their thermoresponsive behavior. Binary mixtures of isotactic poly(**ME**) (*iso*-poly(**ME**)) with dimethyl sulfoxide (DMSO) and with *N,N*-dimethylformamide (DMF) underwent thermoresponsive gel-to-sol transition, in which the mixture turned from gel to sol at a certain temperature as the temperature was increased. On the other hand, aqueous solutions of syndiotactic poly(**ME**) (*syndio*-poly(**ME**)) underwent the LCST-type phase transition, in which the solution was transparent at lower temperatures whereas it became turbid at a certain temperature as the temperature was increased.

Introduction

Polymers, of which physical properties can be controlled in response to external stimuli, have attracted increasing interest from researchers as smart functional materials in recent decades.[1–5] Since the physical properties of polymers depend on the conformation or aggregated state of polymer chains, the control of polymer properties requires marked changes in the conformation or aggregated state of polymer chains that respond to external stimuli. Various stimuli, *e.g.*, temperature, electromagnetic wave, pH, and substances, have been utilized for the control of the physical properties of stimuli-responsive polymers so far.[1–6] Of these stimuli, temperature is the most fundamental and has thus been investigated in the most detail. Typical examples of thermoresponsive polymers reported include (i) lower-critical-solution-temperature (LCST) or upper-critical-solution-temperature (UCST) type phase tran-

sition, in which the solubility of polymer chains in a solvent changes markedly at a critical temperature,[7–21] (ii) thermoresponsive gel-to-sol transition, in which crosslinking density alters remarkably at a certain temperature,[22–26] and (iii) thermoresponsive shape memory behavior, which is based on polymer networks containing thermally non-responsive covalent crosslinks and thermoresponsive noncovalent crosslinks.[27–33] It is an important subject of investigation to develop thermoresponsive polymers with new polymer backbone for expanding their potential because the thermoresponsiveness of polymers should be strongly dependent on their polymer structure.

Copper(I)-catalyzed azide–alkyne cycloaddition (CuAAC) is one of the most important reactions in click chemistry because CuAAC produces selectively and efficiently 1,4-disubstituted 1,2,3-triazole from azide and alkyne moieties in the presence of a copper(I) compound with a wide tolerance for various functional groups.[34–39] Thus, CuAAC has been widely utilized for synthesis of new polymers possessing 1,2,3-triazole moieties in their backbone.[40–53] We have been also working on the synthesis of dense 1,2,3-triazole polymers by CuAAC polymerization of 3-azido-1-propyne derivatives possessing azide and alkyne moieties linked *via* a carbon atom.[54–59] Recently, we prepared a series of dense 1,2,3-triazole polymers carrying amide side chains, aiming at synthesis of new

[a]Department of Macromolecular Science, Graduate School of Science, Osaka University, 1-1 Machikaneyama-cho, Toyonaka, Osaka 560-0043, Japan.
E-mail: hashidzume@chem.sci.osaka-u.ac.jp

[b]Administrative Department, Graduate School of Science, Osaka University, 1-1 Machikaneyama-cho, Toyonaka, Osaka 560-0043, Japan

†Electronic supplementary information (ESI) available. See DOI: https://doi.org/10.1039/d2py01528e

thermoresponsive polymers.[60] The characterization data have demonstrated that poly(*N*-ethyl-*N*-methyl-4-azido-5-hexynamide) (poly(**ME**)) is a new LCST-type thermoresponsive polymer exhibiting a large hysteresis. It should be noted that the fraction of polymer chains that underwent phase separation was only *ca.* 15% of the polymer sample. Since the monomer, *N*-ethyl-*N*-methyl-4-azido-5-hexynamide (**ME**), possesses a chiral carbon on the 4-position and its racemic mixture was used in our previous study, the poly(**ME**) obtained was an atactic polymer (*a*-poly(**ME**)) that possesses a statistical sequence of the *R*- and *S*-isomers. Thus, the poly(**ME**) chains that underwent phase separation should be characterized to elucidate their specific structural features, *e.g.*, molecular weight and stereoregularity.

Among LCST-type thermoresponsive polymers, poly(*N*-isopropylacrylamide) (PNIPAM) has been studied in the most detail by a number of research groups.[61,62] These researches have elucidated that the phase transition temperature for PNIPAM aqueous solutions depends on some structural parameters, *e.g.*, stereoregularity, molecular architecture, and the terminal group. The phase separation temperature for PNIPAM aqueous solutions increases with increasing the fraction of *r*-diad.[63–65] Since PNIPAM is usually prepared by conventional or controlled radical polymerization of a vinyl monomer, NIPAM, it is still difficult to obtain PNIPAM samples of *ca.* 100% *m*- and *r*-diad fractions.[66–73]

In contrast to PNIPAM, the *R*- and *S*-isomers of the monomer (**ME**) precursor of an enantiomer excess (ee) ≥96% can be synthesized through asymmetric reduction (Fig. S1, ESI†).[74,75] Using the *R*- and *S*-isomers of **ME** precursor, it is possible to synthesize optically-pure stereoregular poly(**ME**) by CuAAC polymerization of the stereoregular dimers. In this study, we thus synthesized two types of poly(**ME**) (*i.e.*, isotactic and syndiotactic) by CuAAC polymerization of **ME** dimers of the *R*- and *R*-isomers, and the *R*- and *S*-isomers (the **RR** and **RS** dimers), respectively, and investigated the LCST-type phase transition behavior of their aqueous solutions. It is noteworthy that a gel mixture was obtained in CuAAC polymerization of the **RR** dimer using *N,N*-dimethylformamide (DMF) as a solvent. Thus, the thermoresponsive gelation behavior of isotactic polymer (*iso*-poly(**ME**)) was also investigated in this study.

Results and discussion

Synthesis of stereoregular poly(ME) samples

In this study, two types of stereoregular poly(**ME**) samples were synthesized, *i.e.*, *iso*-poly(**ME**) and *syndio*-poly(**ME**), which are homopolymer of the *R*-isomer and alternating copolymer of the *R*- and *S*-isomers of **ME**, respectively. Both the polymers were prepared by CuAAC polymerization of the corresponding dimers, *i.e.*, the **RR** and **RS** dimers, respectively. The corresponding dimers were synthesized according to Scheme 1. The starting materials in this study, *i.e.*, the *t*-butyldimethylsilyl (TBDMS)-protected stereoregular dimers of *t*-butyl 4-azido-5-hexynoate (tBuAH) (**1RR** and **1RS**), were prepared according to our previous report.[75] The TBDMS-protected tBuAH dimer, **1RR** (or **1RS**), was hydrolyzed with trifluoroacetic acid (TFA) to remove the *t*-butyl groups. The obtained **2RR** (or **2RS**) was coupled with *N*-methylethylamine in the presence of 1-(3-dimethylaminopropyl)-3-ethylcarbodiimide hydrochloride (EDC), 1-hydroxybenzotriazole (HOBt), and diisopropylethylamine (DIPEA) to yield **3RR** (or **3RS**). The TBDMS protecting group of **3RR** (or **3RS**) was removed using tetrabutylammonium fluoride (TBAF) to form the monomer used in this study, *i.e.*, the **RR** (or **RS**) dimer. All the steps proceeded in reasonable yields (*ca.* 60–90%). Both the **RR** and **RS** dimers were fully characterized by ^{1}H and ^{13}C NMR and electrospray ionization-mass spectrometry (ESI-MS) (see Experimental, ESI†). As an example, the ^{1}H NMR spectra of **RR** and **RS** dimers are shown in Fig. 1a and b. These spectra indicate the signals due to the triazole and two methine protons at *ca.* 7.8, 5.7, and 4.8 ppm, respectively. The signals at *ca.* 2.6 ppm are assignable to the ethynyl proton. There are signals due to the methylene protons in the region of 2.2–2.5 ppm. These spectra also contain the signals of *N*-methyl protons at *ca.* 2.9 ppm and the signals due to the *N*-ethyl protons at *ca.* 3.3 and 1.1 ppm. It should be noted here that the signals due to *N*-methyl protons were observed as four singlets, indicating that the amide moieties take both *cis* and *trans* conformations in the dimers.

CuAAC polymerizations of the **RR** and **RS** dimers were carried out in DMF at 60 °C for 48 h using CuBr as a copper(I) catalyst (Scheme 2 and Table S1, ESI†). It is noteworthy that

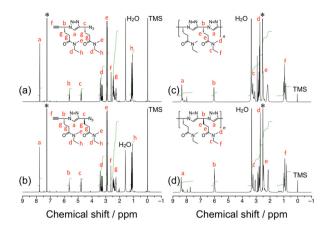**Scheme 1** Synthesis of the **RR** and **RS** dimers of **ME**.

Fig. 1 ^{1}H NMR spectra for the **RR** dimer (a) and **RS** dimer (CDCl$_3$) (b), and for *iso*-poly(**ME**)-2 (c) and *syndio*-poly(**ME**)-3 (DMSO-d_6) (d).

Scheme 2 CuAAC polymerization of the **RR** and **RS** dimers of **ME**.

CuAAC polymerization of the **RR** dimer yielded a gel mixture (Fig. S2, ESI†). Thus, the obtained *iso*-poly(**ME**) was fractionated into water-insoluble and water-soluble parts (*iso*-poly(**ME**)-1 and *iso*-poly(**ME**)-2, respectively). The total yield of two fractions of *iso*-poly(**ME**) was 67%. The samples of *syndio*-poly(**ME**) were obtained after reprecipitation using DMF and

diethyl ether as good and poor solvents, as in the case of CuAAC polymerization of racemic **ME** monomer.[60] The *syndio*-poly(**ME**) samples were obtained in modest yields (52–77%). It is known that the yield of CuAAC depends on the reaction conditions, *i.e.*, substrates, solvent, copper(I) catalyst, temperature, and additive.[37–39] In this study, however, the conditions of CuAAC polymerization were not fully optimized because only limited amounts of the **RR** and **RS** dimers were obtained. It is difficult to remove completely copper ions from dense 1,2,3-triazole polymers even by washing with an aqueous solution of ethylenediaminetetraacetic acid (EDTA),[54,58,60] In this study, the amount of residual copper ions were roughly estimated for the polymer samples by elemental analysis (see Experimental, ESI†).

Two samples of *iso*-poly(**ME**) and three samples of *syndio*-poly(**ME**) were utilized in this study. Table S1 in ESI† summarizes the M_w and M_w/M_n values estimated for the poly(**ME**) samples by size exclusion chromatography (SEC) calibrated with standard samples of poly(ethylene glycol) (PEG) and poly(ethylene oxide) (PEO). The M_w values for *iso*-poly(**ME**)-1, *iso*-poly(**ME**)-2, *syndio*-poly(**ME**)-1, *syndio*-poly(**ME**)-2, and *syndio*-poly(**ME**)-3 were 1.8×10^4, 1.8×10^3, 9.1×10^3, 6.6×10^3, and 2.5×10^3, respectively (see also Fig. S3, ESI†). Fig. 1c and d display ^{1}H NMR spectra for *iso*-poly(**ME**)-2 and *syndio*-poly(**ME**)-3. The spectra contain the signals assignable to triazole and methine protons in the backbone at *ca.* 8.4 and 6.0 ppm, respectively. The signals in the region of 2.1–2.5 ppm are ascribable to the methylene protons. The spectra also indicate the signals of *N*-methyl protons at *ca.* 2.8 ppm and the signals due to the *N*-ethyl protons at *ca.* 3.3 and 0.9 ppm. These data are indicative of successful synthesis of the *iso*-poly(**ME**) and *syndio*-poly(**ME**) samples. As can be seen in Fig. S4 in ESI,† the circular dichroism (CD) spectrum for *iso*-poly(**ME**) shows a significant positive signal whereas that for *syndio*-poly(**ME**) does not contain any significant signals. The solubility of the obtained polymer samples in various solvents was tested (Table 1). This table also contains the data for poly(**ME**) of M_w

Table 1 Results of solubility tests of *a*-poly(**ME**), *iso*-poly(**ME**)-1, *iso*-poly(**ME**)-2, *syndio*-poly(**ME**)-1, *syndio*-poly(**ME**)-2, and *syndio*-poly(**ME**)-3^a

Solvent	*a*-Poly(ME)^b	*iso*-Poly(ME)-1^c	*iso*-Poly(ME)-2	*syndio*-Poly(ME)-1	*syndio*-Poly(ME)-2	*syndio*-Poly(ME)-3
Water^d	++	−	++	++	++	++
Methanol	++	−	++	++	++	++
Ethanol	++	−	++	++	++	++
2-Propanol	−	−	+	−	−	−
DMSO	++	++	++	++	++	++
DMF	++	++	++	++	++	++
Acetonitrile	++	−	++	++	++	++
Acetone	−	−	++	++	++	++
Ethyl acetate	−	−	−	−	−	−
THF	−	−	+	−	−	−
Chloroform	++	−	++	++	++	++
DCM	++	−	++	++	++	++
Toluene	−	−	−	−	−	−
Diethyl ether	−	−	−	−	−	−
Hexane	−	−	−	−	−	−

^{a} "++", "+", and "−" denote soluble at ≥10 g L^{-1}, ≥1 g L^{-1}, and insoluble, respectively. ^{b} Data from Ref. 60. ^{c} At a temperature close to the boiling point. ^{d} At *ca.* 0 °C.

= 7.1×10^3 obtained by CuAAC polymerization of racemic **ME** (*a*-poly(**ME**)) for comparison.[60] *iso*-Poly(**ME**)-2, *syndio*-poly(**ME**)-1, *syndio*-poly(**ME**)-2, and *syndio*-poly(**ME**)-3 exhibit almost the same solubilities as those of *a*-poly(**ME**); These four samples were soluble in many solvents, *e.g.*, water, methanol, ethanol, dimethyl sulfoxide (DMSO), DMF, acetonitrile, chloroform, and DCM, but insoluble in ethyl acetate, toluene, diethyl ether, and hexane. On the other hand, *iso*-poly(**ME**)-1 was soluble only in DMSO and DMF at higher temperatures presumably because of the higher M_w.

Thermoresponsive gel-to-sol transition

Since the CuAAC polymerization of the **RR** dimer yielded a gel mixture as described above, the thermoresponsive gelation behavior of *iso*-poly(**ME**)-1 was investigated using DMSO and DMF as solvent. The sample solutions of *iso*-poly(**ME**)-1 were prepared using DMSO and DMF, respectively, at higher temperatures. These binary mixtures turned gel at lower temperatures, as can be seen in Fig. 2a. These observations indicate that extended network structures were formed through noncovalent crosslinking between *iso*-poly(**ME**) chains at low temperatures. Since gelation was not observed for any binary mixtures of *a*-poly(**ME**) or *syndio*-poly(**ME**) with DMSO or DMF, it is likely that this gelation is based on longer sequences of the *R*-isomer units. As can be seen in Fig. S5 in ESI,† the powder X-ray diffraction pattern (PXRD) for *iso*-poly(**ME**)-1 exhibits resolved peaks, indicating that *iso*-poly(**ME**)-1 is crystalline. It is thus likely that the crosslinks in the binary gel mixtures are based on the partial crystallization of longer *iso*-poly(**ME**)-1 chains. Fig. 2b displays the gel-to-sol transition temperature (T_{sol}) determined by the sample inversion method for binary mixtures of varying polymer concentrations (C). In the case of the *iso*-poly(**ME**)-1/DMSO binary mixture, T_{sol} increased from 52 to 130 °C with increasing C from 1.2 to 4.9 wt%. In the case of the *iso*-poly(**ME**)-1/DMF binary mixture, on the other hand, T_{sol} increased only slightly from 103 to 114 °C with increasing C from 1.1 to 7.3 wt%. These observations indicate that the temperature dependencies of solubility of *iso*-poly(**ME**)-1 in the solvents should be different because T_{sol} should be lower for a better solvent. Both DMSO and DMF are aprotic polar solvents that dissolve well the dense 1,2,3-triazole polymers we prepared so far. These solvents may also exhibit a higher affinity for the *N*-ethyl-*N*-methylamide side chains of poly(**ME**) because of the larger dielectric constants (47.24 and 38.25 for DMSO and DMF, respectively, at 20 °C).[76] At present, we do not have any reasonable explanations for the difference in gelation behavior of *iso*-poly(**ME**)-1 in DMSO and DMF, *i.e.*, the C dependency of T_{sol}.

Lower-critical-solution-temperature-type phase transition

Since our previous study has demonstrated that *a*-poly(**ME**) is an LCST-type thrmoresponsive polymer,[60] the phase transition behavior of aqueous solutions of the water-soluble samples, *i.e.*, *iso*-poly(**ME**)-2, *syndio*-poly(**ME**)-1, and *syndio*-poly(**ME**)-3, was investigated. Fig. 3a demonstrates photographs for
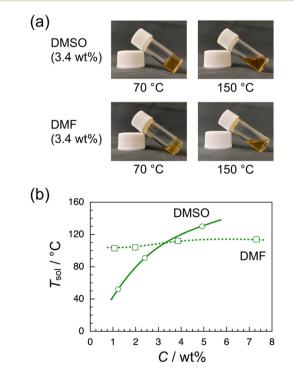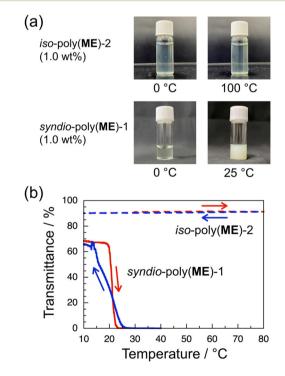

Fig. 2 Photographs for binary mixtures of *iso*-poly(ME)-1/DMSO and *iso*-poly(ME)-1/DMF at 70 and 150 °C (a) and T_{sol} as a function of C for the *iso*-poly(ME)-1/DMSO (circle) and *iso*-poly(ME)-1/DMF binary mixtures (square) (b).

Fig. 3 Photographs for 1.0 wt% aqueous solutions of *iso*-poly(ME)-2 and *syndio*-poly(ME)-1 at lower and higher temperatures (a) and transmittance data for 1.0 wt% aqueous solutions of *iso*-poly(ME)-2 (broken lines) and *syndio*-poly(ME)-1 (solid lines) monitored at 510 nm with heating (red) and cooling (blue) at 1.0 and 0.30 °C min⁻¹, respectively (b).

1.0 wt% aqueous solutions of *iso*-poly(**ME**)-2 (upper) and *syndio*-poly(**ME**)-1 (lower). The bluish green color of the *iso*-poly(**ME**)-2 aqueous solution was due to the residual copper ions. The aqueous solution of *iso*-poly(**ME**)-2 exhibited almost the same appearance at 0 and 100 °C. On the other hand, the aqueous solution of *syndio*-poly(**ME**)-1 was rather transparent at 0 °C whereas it was strongly turbid at 25 °C. These observations indicate that the aqueous solution of *syndio*-poly(**ME**)-1 underwent the LCST-type phase separation whereas the aqueous solution of *iso*-poly(**ME**)-2 did not. As can be seen in Fig. 3b, the transmittance data were monitored for the 1.0 wt% aqueous solutions of *iso*-poly(**ME**)-2 and *syndio*-poly(**ME**)-1 at 510 nm, at which the transmittance was close to the maximum at lower temperatures, with heating and cooling at 1.0 and 0.30 °C min^{-1}, respectively. The transmittance of the aqueous solution of *iso*-poly(**ME**)-2 was almost constant at *ca.* 90% in the temperature range of 10–80 °C. On the other hand, as the temperature was increased from 10 to 40 °C at 0.30 °C min^{-1}, the transmittance of the aqueous solution of *syndio*-poly(**ME**)-1 decreased abruptly from *ca.* 70% to 0% in a narrow temperature region of 22–23 °C. In the cooling process at 0.30 °C min^{-1}, the transmittance for the *syndio*-poly(**ME**)-1 solution started to increase gradually at *ca.* 25 °C and recovered to the initial value at *ca.* 15 °C. (The transmittance was unstable in the region of 20–16 °C in the cooling process.) It should be noted here that the hysteresis observed for the aqueous solution of *syndio*-poly(**ME**)-1 in this study is different from the conventional one; The transmittance recovers in the cooling process in a temperature region lower than that of the transmittance decrease in the heating process.

It is noteworthy that the transmittance data for the *syndio*-poly(**ME**)-1 solution were strongly dependent on the heating and cooling rates. The broken lines in Fig. 4a show the transmittance data obtained for a 1.0 wt% aqueous solution of *syndio*-poly(**ME**)-1 with heating and cooling at 3.0, 2.0, 1.0, 0.50, and 0.30 °C min^{-1}. At heating and cooling rates of 3.0, 2.0, 1.0, and 0.50 °C min^{-1}, the transmittance decreased abruptly at a certain temperature between *ca.* 22 and 23 °C in the heating process, whereas the transmittance commenced to increase at a certain temperature between *ca.* 21 and 20 °C in the cooling process, indicative of normal hysteresis. In the cooling process at 0.30 °C min^{-1}, on the other hand, the transmittance started to recover at *ca.* 25 °C, which was higher than the temperature range of decrease in transmittance in the heating process. The clouding and clearing point temperatures (T_{cloud} and T_{clear}, respectively) were roughly estimated as the temperature at which the transmittance took half of the initial value of heating process, and plotted in Fig. 4b against the heating or cooling rate. This figure indicates that as the heating or cooling rate was decreased from 3.0 to 0.30 °C min^{-1}, T_{cloud} decreased gradually from *ca.* 24 to 21 °C whereas T_{clear} increased gradually from *ca.* 13 to 15 °C in a range of 3.0–0.50 °C min^{-1}, and then increased markedly to 20 °C in a narrow range of 0.50–0.30 °C min^{-1}.

Since *syndio*-poly(**ME**)-1 sample contained a small amount of residual copper ions (see Experimental, ESI†), the copper
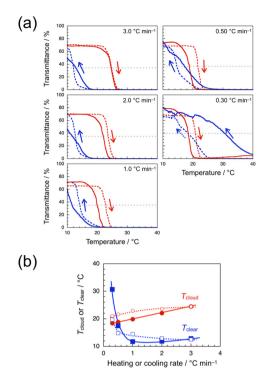

Fig. 4 Transmittance data for a 1.0 wt% aqueous solution of *syndio*-poly(**ME**)-1 before (broken lines) and after treatment with 3-mercaptopropyl silica gel (solid lines) monitored at 510 nm with heating (red) and cooling (blue) at 3.0, 2.0, 1.0, 0.50, and 0.30 °C min^{-1} (a), and T_{cloud} (red circle) and T_{clear} (blue square) as a function of the heating and cooling rate determined for the 1.0 wt% aqueous solution of *syndio*-poly(**ME**)-1 before (unfilled symbols) and after treatment with 3-mercaptopropyl silica gel (filled symbols) in the heating and cooling process, respectively (b).

ions might cause the unique hysteresis observed in the slow heating and cooling processes.[77] Thus, the sample was treated with 3-mercaptopyropyl silica gel. It was not possible to remove all the residual copper ions, but a *syndio*-poly(**ME**)-1 sample with *ca.* 25% copper ions removed was recovered. The transmittance data were recorded for a 1.0 wt% aqueous solution of the *syndio*-poly(**ME**)-1 sample treated (solid lines in Fig. 4a). When the temperature was increased and decreased at 3.0 °C min^{-1}, the transmittance data were practically identical to those of the untreated sample. In the heating process at 2.0 or 1.0 °C min^{-1}, the transmittance decreased in a lower temperature range than that for the untreated sample. In the cooling process at 2.0 or 1.0 °C min^{-1}, the transmittance started to increase at *ca.* 20 °C, which was almost the same as that for the untreated sample, but the transmittance recovered more slowly and did not reach the initial value at 10 °C. The unique hysteresis was observed at heating and cooling rate of 0.50 °C min^{-1}; The transmittance decreased in a wider temperature range of *ca.* 15–20 °C in the heating process, whereas the transmittance started to increase at *ca.* 26 °C in the cooling process and then recovered gradually to the initial value at 10 °C. It is noteworthy that the effect of copper ions was more pronounced in the slower heating and cooling processes at 0.30 °C min^{-1}. In the heating process, the transmit-

tance decreased from *ca.* 80% to 0% in the temperature range of 15–21 °C, and then increased slightly to 4% in a higher temperature range of 25–40 °C. In the subsequent cooling process, the transmittance gradually recovered from *ca.* 7% as the temperature was decreased from 40 °C and returned the initial value at 10 °C. These observations are indicative of inverse hysteresis. T_{cloud} and T_{clear} were also roughly estimated and plotted in Fig. 4b against the heating or cooling rate. As the heating or cooling rate was decreased from 3.0 to 0.10 °C min^{-1}, T_{cloud} decreased gradually from *ca.* 24 to 18 °C whereas T_{clear} decreased slightly from *ca.* 13 to 12 °C in a range of 3.0–1.0 °C min^{-1}, and then increased markedly to *ca.* 31 °C in a range of 1.0–0.30 °C min^{-1}.

The transmittance data were also obtained for a 1.0 wt% aqueous solution of *syndio*-poly(**ME**)-3 of M_w lower than that of *syndio*-poly(**ME**)-1. Fig. 5a shows the transmittance data obtained for a 1.0 wt% aqueous solution of *syndio*-poly(**ME**)-3 with heating and cooling at 3.0, 2.0, 1.0, 0.40, and 0.10 °C min^{-1}. In the faster heating and cooling processes at 3.0 and 2.0 °C min^{-1}, the transmittance data are indicative of normal hysteresis. In the slower heating and cooling processes at 1.0, 0.40, and 0.10 °C min^{-1}, on the other hand, the transmittance data indicate inverse hysteresis. These observations indicate that shorter chains of *syndio*-poly(**ME**) are rearranged more easily in polymer aggregates formed at higher temperatures.
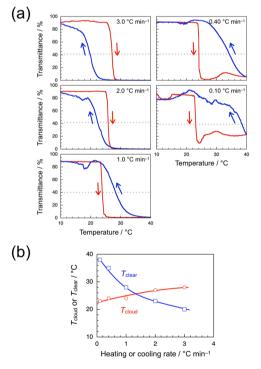
T_{cloud} and T_{clear} were also plotted in Fig. 5b against the heating or cooling rate. This figure indicates that as the heating or cooling rate was decreased from 3.0 to 0.10 °C min^{-1}, T_{cloud} decreased gradually from 28 to 23 °C whereas T_{clear} increased gradually from 20 to 38 °C.

The LCST-type phase transition behavior for aqueous solutions of *syndio*-poly(**ME**)-3 was also investigated by ^{1}H NMR and differential scanning calorimetry (DSC). Fig. 6 displays ^{1}H NMR spectra recorded for a 1.0 wt% solution of *syndio*-poly(**ME**)-3 in D$_2$O at different temperatures, *i.e.*, 20, 40, 60, and 80 °C. Here the temperature was increased to the measurement temperature in a few minutes and then the sample solution was equilibrated. As can be seen in Fig. 6c and d, new signals ascribable to the triazole and methine protons were observed in lower magnetic fields at higher temperatures, *i.e.*, 60 and 80 °C. These signals are likely ascribed to more hydrated polymer chains in aggregates. The fraction of more hydrated polymer chain was roughly estimated to be *ca.* 28% at 80 °C from the area intensities of signals due to the triazole protons. Fig. S6 in ESI† shows the DSC data obtained for a 1.0 wt% aqueous solution of *syndio*-poly(**ME**)-3 at heating and cooling rates of 1.0 °C min^{-1}. The DSC data did not exhibit any significant signals ascribable to the LCST-type phase transition of aqueous solution of *syndio*-poly(**ME**)-3 in the heating or cooling process, similar to the case of *a*-poly(**ME**).[60] These observations indicate that only a small fraction of polymer chains underwent the phase transition or the phase transition of aqueous *syndio*-poly(**ME**) solution caused only small calorimetric changes.

In LCST-type phase transition of aqueous solutions of thermoresponsive polymers, hysteresis is often observed; Once
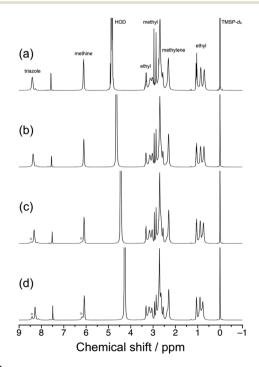

Fig. 5 Transmittance data for a 1.0 wt% aqueous solution of *syndio*-poly(**ME**)-3 monitored at 510 nm with heating (red) and cooling (blue) at 3.0, 2.0, 1.0, 0.40, and 0.10 °C min^{-1} (a), and T_{cloud} (red circle) and T_{clear} (blue square) as a function of the heating and cooling rate determined for the 1.0 wt% aqueous solution of *syndio*-poly(**ME**)-3 solution in the heating and cooling process, respectively (b).

Fig. 6 ^{1}H NMR spectra for a 1.0 wt% solution of *syndio*-poly(**ME**)-3 in D$_2$O measured at 20 (a), 40 (b), 60 (c), and 80 °C (d).

the phase separation occurs at higher temperatures, the transmittance recovers in the cooling process in the temperature region lower than the region in which the transmittance decreases in the heating process. The normal hysteresis is likely caused by slow rehydration in the cooling process presumably because of the restricted mobility of polymer chains in aggregates. To the best of our knowledge, there have been only a few examples of inverse hysteresis in the LCST-type phase transition.[77,78] Yeshchenko *et al.*,[77] reported that aqueous solutions containing a dextran-graft-PNIPAM copolymer and gold nanoparticles (AuNPs) underwent an LCST-type phase transition exhibiting inverse hysteresis. The authors concluded that AuNPs counteracted the formation of PNIPAM aggregates. In this study, aqueous solutions of *syndio*-poly(**ME**) samples underwent the LCST-type phase separation. The phase separation behavior depended on the heating and cooling rates, the amount of residual copper ions, and the molecular weight. It is noteworthy that inverse hysteresis was observed in the slow heating and cooling processes for a *syndio*-poly(**ME**) sample containing a smaller amount of residual copper ions or possessing a lower molecular weight. In the heating process, where the clear inverse hysteresis was observed, the transmittance increased slightly in a higher temperature region after phase separation occurred. It is likely that *syndio*-poly(**ME**) chains are rearranged in polymer aggregates during the slight increase in transmittance, resulting in the formation of polymer aggregates which are more readily rehydrated. Since the conformational change might occur rather slowly, the inverse hysteresis was observed only in slower processes. The residual copper ions inhibit the conformational change presumably because of coordination to the 1,2,3-triazole moieties and amide side chains in polymer chains.[38,79] *syndio*-Poly(**ME**) chains of lower molecular weights undergo more easily the conformational change. It should be noted here that the inverse hysteresis was not observed for any aqueous solutions of *a*-poly(**ME**) samples. It is thus likely that the syndiotactic sequence, *i.e.*, the alternating sequence of the *R*- and *S*-isomers of **ME**, which is longer than a critical length, is necessary for the inverse hysteresis. The LCST-type phase separation behavior of aqueous solutions of uniform oligomers of *syndio*-poly(**ME**) will be further investigated to elucidate the molecular mechanism of inverse hysteresis in near future.

Conclusions

In this study, two types of stereoregular poly(**ME**) samples, *i.e.*, *iso*-poly(**ME**) and *syndio*-poly(**ME**), were synthesized by CuAAC polymerization of the **RR** and **RS** dimers, respectively. Since the CuAAC polymerization of the **RR** dimer yielded a gel mixture, the obtained *iso*-poly(**ME**) was fractionated into water-insoluble and water-soluble parts, *i.e.*, *iso*-poly(**ME**)-1 ($M_w = 1.8 \times 10^4$) and *iso*-poly(**ME**)-2 ($M_w = 1.8 \times 10^3$), respectively. On the other hand, the three samples of *syndio*-poly(**ME**) (*syndio*-poly(**ME**)-1 ($M_w = 9.1 \times 10^3$), *syndio*-poly(**ME**)-2 ($M_w = 6.6 \times 10^3$), and

syndio-poly(**ME**)-3 ($M_w = 2.5 \times 10^3$)) were obtained after reprecipitation using DMF and diethyl ether as good and poor solvents. The poly(**ME**) samples used in this study contained a small amount of residual copper ions, because the dense 1,2,3-triazole backbones usually adsorb strongly copper ions. The thermoresponsive gel-to-sol transition behavior was investigated for *iso*-poly(**ME**)-1 using DMSO and DMF as solvent. The *iso*-poly(**ME**)-1/DMSO and *iso*-poly(**ME**)-1/DMF binary mixtures were gel at lower temperatures whereas the mixtures turned sol at a certain temperature as the temperature was increased, indicating that extended network structures were formed through noncovalent crosslinking between *iso*-poly(**ME**) chains at low temperatures, *e.g.*, partial crystallization. The temperature-dependent transmittance data for aqueous solutions of *iso*-poly(**ME**)-2, *syndio*-poly(**ME**)-1, and *syndio*-poly(**ME**)-3 demonstrated that the *syndio*-poly(**ME**) samples were LCST-type thermoresponsive polymers whereas *iso*-poly(**ME**)-2 was not. The LCST-type phase separation behavior of aqueous solutions of the *syndio*-poly(**ME**) samples depended on the heating and cooling rates, the amount of residual copper ions, and the molecular weight. The noteworthy is that inverse hysteresis was observed in slow heating and cooling processes for a *syndio*-poly(**ME**) sample containing a smaller amount of residual copper ions or possessing a lower molecular weight. In the heating process of inverse hysteresis, the transmittance increased slightly in a higher temperature region after phase separation occurred. It is likely that *syndio*-poly(**ME**) chains are rearranged in polymer aggregates during the slight increase in transmittance, resulting in the formation of polymer aggregates which are more readily rehydrated.

Author contributions

A. H. supervised the project; A. H., Y. K. and K. O. designed the project; K. O., J. M., S. Y. and M. N. performed the experiments; A. H., M. N. and K. O. analyzed data; A. H., Y. K., M. N. and K. O. discussed the results; A. H. and K. O. wrote the paper.

Conflicts of interest

There are no conflicts to declare.

Acknowledgements

References

1 *Handbook of Stimuli-Responsive Materials*, ed. M. W. Urban, Wiley-VCH, Weinheim, Germany, 2011.

2 F. Liu and M. W. Urban, *Prog. Polym. Sci.*, 2010, **35**, 3–23.

3 D. Roy, J. N. Cambre and B. S. Sumerlin, *Prog. Polym. Sci.*, 2010, **35**, 278–301.

4 E. Fleige, M. A. Quadir and R. Haag, *Adv. Drug Delivery Rev.*, 2012, **64**, 866–884.

5 S. Wang, Q. Liu, L. Li and M. W. Urban, *Macromol. Rapid Commun.*, 2021, **42**, 2100054.

6 A. Hashidzume and A. Harada, in *Supramolecular Polymer Chemistry*, ed. A. Harada, Wiley-VCH, Weinheim, Germany, 2012, pp. 231–267.

7 A. Laukkanen, L. Valtola, F. M. Winnik and H. Tenhu, *Macromolecules*, 2004, **37**, 2268–2274.

8 S. Aoshima and S. Kanaoka, *Adv. Polym. Sci.*, 2008, **210**, 169–208.

9 N. S. Ieong, M. Hasan, D. J. Phillips, Y. Saaka, R. K. O'Reilly and M. I. Gibson, *Polym. Chem.*, 2012, **3**, 794–799.

10 C. Weber, R. Hoogenboom and U. S. Schubert, *Prog. Polym. Sci.*, 2012, **37**, 686–714.

11 G. Vancoillie, D. Frank and R. Hoogenboom, *Prog. Polym. Sci.*, 2014, **39**, 1074–1095.

12 Y. Kohno, S. Saita, Y. Men, J. Yuan and H. Ohno, *Polym. Chem.*, 2015, **6**, 2163–2178.

13 J. C. Foster, I. Akar, M. C. Grocott, A. K. Pearce, R. T. Mathers and R. K. O'Reilly, *ACS Macro Lett.*, 2020, **9**, 1700–1707.

14 D. N. Schulz, D. G. Peiffer, P. K. Agarwal, J. Larabee, J. J. Kaladas, L. Soni, B. Handwerker and R. T. Garner, *Polymer*, 1986, **27**, 1734–1742.

15 J. Seuring and S. Agarwal, *Macromolecules*, 2012, **45**, 3910–3918.

16 J. Seuring and S. Agarwal, *Macromol. Rapid Commun.*, 2012, **33**, 1898–1920.

17 J. Seuring and S. Agarwal, *ACS Macro Lett.*, 2013, **2**, 597–600.

18 Q. Zhang and R. Hoogenboom, *Prog. Polym. Sci.*, 2015, **48**, 122–142.

19 J. Niskanen and H. Tenhu, *Polym. Chem.*, 2017, **8**, 220–232.

20 Z. Xu and W. Liu, *Chem. Commun.*, 2018, **54**, 10540–10553.

21 C. M. Papadakis, P. Müller-Buschbaum and A. Laschewsky, *Langmuir*, 2019, **35**, 9660–9676.

22 M. R. Matanović, J. Kristl and P. A. Grabnar, *Int. J. Pharm.*, 2014, **472**, 262–275.

23 A. P. Constantinou and T. K. Georgiou, *Eur. Polym. J.*, 2016, **78**, 366–375.

24 M. J. Taylor, P. Tomlins and T. S. Sahota, *Gels*, 2017, **3**, 4.

25 S. Chatterjee, P. C. Hui and C.-w. Kan, *Polymers*, 2018, **10**, 480.

26 K. Zhang, K. Xue and X. J. Loh, *Gels*, 2021, **7**, 77.

27 Y. Osada and A. Matsuda, *Nature*, 1995, **376**, 219.

28 A. Lendlein and S. Kelch, *Angew. Chem., Int. Ed.*, 2002, **41**, 2034–2057.

29 A. Garle, S. Kong, U. Ojha and B. M. Budhlall, *ACS Appl. Mater. Interfaces*, 2012, **4**, 645–657.

30 Q. Zhao, M. Behl and A. Lendlein, *Soft Matter*, 2013, **9**, 1744–1755.

31 Y. Liu, Y. Li, G. Yang, X. Zheng and S. Zhou, *ACS Appl. Mater. Interfaces*, 2015, **7**, 4118–4126.

32 B. Q. Y. Chan, S. J. W. Heng, S. S. Liow, K. Zhang and X. J. Loh, *Mater. Chem. Front.*, 2017, **1**, 767–779.

33 Y. Xia, Y. He, F. Zhang, Y. Liu and J. Leng, *Adv. Mater.*, 2021, **33**, 2000713.

34 C. W. Tornøe, C. Christensen and M. Meldal, *J. Org. Chem.*, 2002, **67**, 3057–3064.

35 V. V. Rostovtsev, L. G. Green, V. V. Fokin and K. B. Sharpless, *Angew. Chem., Int. Ed.*, 2002, **41**, 2596–2599.

36 F. Fazio, M. C. Bryan, O. Blixt, J. C. Paulson and C.-H. Wong, *J. Am. Chem. Soc.*, 2002, **124**, 14397–14402.

37 *Click Chemistry for Biotechnology and Materials Science*, ed. J. Lahann, Wiley & Sons, Chichester, UK, 2009.

38 *Click Triazoles*, ed. J. Košmrlj, Springer, Heidelberg, Germany, 2012.

39 *Chemistry of 1,2,3-Triazoles*, ed. W. Dehaen and V. A. Bakulev, Springer, Cham, Switzerland, 2015.

40 B. Le Droumaguet and K. Velonia, *Macromol. Rapid Commun.*, 2008, **29**, 1073–1089.

41 M. Meldal, *Macromol. Rapid Commun.*, 2008, **29**, 1016–1051.

42 J. A. Johnson, M. G. Finn, J. T. Koberstein and N. J. Turro, *Macromol. Rapid Commun.*, 2008, **29**, 1052–1072.

43 A. Qin, J. W. Y. Lam and B. Z. Tang, *Macromolecules*, 2010, **43**, 8693–8702.

44 A. Qin, J. W. Y. Lam and B. Z. Tang, *Chem. Soc. Rev.*, 2010, **39**, 2522–2544.

45 *Click Polymerization*, A. Qin and B. Z. Tang, ed. Royal Society of Chemistry, London, UK, 2018.

46 J. A. F. Joosten, N. T. H. Tholen, F. Ait El Maate, A. J. Brouwer, G. W. van Esse, D. T. S. Rijkers, R. M. J. Liskamp and R. J. Pieters, *Eur. J. Org. Chem.*, 2005, 3182–3185.

47 M. van Dijk, M. L. Nollet, P. Weijers, A. C. Dechesne, C. F. van Nostrum, W. E. Hennink, D. T. S. Rijkers and R. M. J. Liskamp, *Biomacromolecules*, 2008, **9**, 2834–2843.

48 S. van der Wal, C. J. Capicciotti, S. Rontogianni, R. N. Ben and R. M. J. Liskamp, *MedChemComm*, 2014, **5**, 1159–1165.

49 S. Binauld, F. Boisson, T. Hamaide, J.-P. Pascault, E. Drockenmuller and E. Fleury, *J. Polym. Sci., Part A: Polym. Chem.*, 2008, **46**, 5506–5517.

50 C. Besset, S. Binauld, M. Ibert, P. Fuertes, J.-P. Pascault, E. Fleury, J. Bernard and E. Drockenmuller, *Macromolecules*, 2010, **43**, 17–19.

51 M. M. Obadia and E. Drockenmuller, *Chem. Commun.*, 2016, **52**, 2433–2450.

52 O. D. Montagnat, G. Lessene and A. B. Hughes, *J. Org. Chem.*, 2010, **75**, 390–398.

53 O. D. Montagnat, G. Lessene and A. B. Hughes, *Aust. J. Chem.*, 2010, **63**, 1541–1549.

54 A. Hashidzume, T. Nakamura and T. Sato, *Polymer*, 2013, **54**, 3448–3451.

55 Y. Yang, A. Mori and A. Hashidzume, *Polymers*, 2019, **11**, 1086.

56 Y. Yang and A. Hashidzume, *Macromol. Chem. Phys.*, 2019, **220**, 1900317.

57 Y. Yang, Y. Kamon, N. A. Lynd and A. Hashidzume, *Macromolecules*, 2020, **53**, 10323–10329.

58 S. Yamasaki, Y. Kamon, L. Xu and A. Hashidzume, *Polymers*, 2021, **13**, 1627.

59 L. Xu, Y. Kamon and A. Hashidzume, *Polymers*, 2021, **13**, 1614.

60 K. Okuno, T. Arisawa, Y. Kamon, A. Hashidzume and F. M. Winnik, *Langmuir*, 2022, **38**, 5156–5165.

61 H. G. Schild, *Prog. Polym. Sci.*, 1992, **17**, 163–249.

62 A. Halperin, M. Kröger and F. M. Winnik, *Angew. Chem., Int. Ed.*, 2015, **54**, 15342–15367.

63 C. S. Biswas, K. Mitra, S. Singh and B. Ray, *J. Chem. Sci.*, 2016, **128**, 415–420.

64 T. Tada, T. Hirano, K. Ute, Y. Katsumoto, T.-A. Asoh, T. Shoji, N. Kitamura and Y. Tsuboi, *J. Phys. Chem. B*, 2016, **120**, 7724–7730.

65 K. Ushiro, T. Shoji, M. Matsumoto, T.-A. Asoh, H. Horibe, Y. Katsumoto and Y. Tsuboi, *J. Phys. Chem. B*, 2020, **124**, 8454–8463.

66 B. Ray, Y. Isobe, K. Morioka, S. Habaue, Y. Okamoto, M. Kamigaito and M. Sawamoto, *Macromolecules*, 2003, **36**, 543–545.

67 B. Ray, Y. Isobe, K. Matsumoto, S. Habaue, Y. Okamoto, M. Kamigaito and M. Sawamoto, *Macromolecules*, 2004, **37**, 1702–1710.

68 T. Hirano, S. Ishii, H. Kitajima, M. Seno and T. Sato, *J. Polym. Sci., Part A: Polym. Chem.*, 2005, **43**, 50–62.

69 T. Hirano, H. Ishizu, M. Seno and T. Sato, *Polymer*, 2005, **46**, 10607–10610.

70 T. Hirano, H. Kitajima, S. Ishii, M. Seno and T. Sato, *J. Polym. Sci., Part A: Polym. Chem.*, 2005, **43**, 3899–3908.

71 T. Hirano, H. Kitajima, M. Seno and T. Sato, *Polymer*, 2006, **47**, 539–546.

72 T. Hirano, H. Ishizu and T. Sato, *Polymer*, 2008, **49**, 438–445.

73 T. Hirano, T. Kamikubo, Y. Fujioka and T. Sato, *Eur. Polym. J.*, 2008, **44**, 1053–1059.

74 K. Matsumura, S. Hashiguchi, T. Ikariya and R. Noyori, *J. Am. Chem. Soc.*, 1997, **119**, 8738–8739.

75 Y. Kamon, J. Miura, K. Okuno, M. Nakahata and A. Hashidzume, *Macromolecules*, 2023, **56**, 292–304.

76 *Lange's Handbook of Chemistry*, ed. J. A. Dean, McGraw-Hill, New York, 1999, pp. 5105–5128.

77 O. A. Yeshchenko, A. P. Naumenko, N. V. Kutsevol, D. O. Maskova, I. I. Harahuts, V. A. Chumachenko and A. I. Marinin, *J. Phys. Chem. C*, 2018, **122**, 8003–8010.

78 P. Werner, M. Münzberg, R. Hass and O. Reich, *Anal. Bioanal. Chem.*, 2017, **409**, 807–819.

79 O. Clement, B. M. Rapko and B. P. Hay, *Coord. Chem. Rev.*, 1998, **170**, 203–243.